



**Synthesis of [7]Phenacene Incorporating Tetradecyl Chains
in the Axis Positions and Its Application toward Field-effect
Transistor**

Journal:	<i>Journal of Materials Chemistry C</i>
Manuscript ID	TC-ART-01-2020-000272.R2
Article Type:	Paper
Date Submitted by the Author:	14-Apr-2020
Complete List of Authors:	Okamoto, Hideki; Okayama University, Chemistry Hamao, Shino; Okayama University, Research Laboratory for Surface Science Kozasa, Keiko; Okayama University, Chemistry Wang, Yanan; Okayama University, Research Laboratory for Surface Science Kubozono, Yoshihiro; Okayama University, Research Institute for Interdisciplinary Science Pan, Yong-He; National Tsing Hua University Yen, Yu-Hsiung; National Tsing Hua University Hoffmann, Germar; National Tsing Hua University, Department of Physics Tani, Fumito; Kyushu University, Institute for Materials Chemistry and Engineering Goto, Kenta; Kyushu University Institute for Materials Chemistry and Engineering

Synthesis of [7]Phenacene Incorporating Tetradecyl Chains in the Axis Positions and Its Application toward Field-effect Transistor

Hideki Okamoto^{a,*}, Shino Hamao^b, Keiko Kozasa^a, Yanan Wang^b, Yoshihiro Kubozono^{b,*}, Yong-He Pan^c, Yu-Hsiung Yen^c, Germar Hoffmann^c, Fumito Tani^d, and Kenta Goto^d

^a Division of Earth, Life, and Molecular Sciences, Graduate School of Natural Science and Technology, Okayama University, Okayama 700-8530, Japan

^b Research Institute for Interdisciplinary Science, Okayama University, Okayama 700-8530, Japan

^c Department of Physics & Center for Quantum Technology, National Tsing Hua University, Hsinchu 30013, Taiwan

^d Institute for Materials Chemistry and Engineering, Kyushu University, Fukuoka 819-0395, Japan

Abstract

Field-effect transistors (FETs) were fabricated using a new type of phenacene molecule, 3,12-ditetradecyl[7]phenacene ($(C_{14}H_{29})_2$ -[7]phenacene), and solid gate dielectrics or an electric double layer (EDL) capacitor with an ionic liquid (1-butyl-3-methylimidazolium hexafluorophosphate (bmim[PF₆])). The new molecule, $(C_{14}H_{29})_2$ -[7]phenacene, was efficiently synthesized via the Mallory photoreaction. Its crystal structure and electronic properties were determined, using X-ray diffraction, scanning tunneling microscopy / spectroscopy (STM and STS), absorption spectroscopy, and photoelectron yield spectroscopy, which showed a monoclinic crystal lattice (space group $P2_1$ (No. 4)) and an energy gap of ~ 3.0 eV. The STM image clearly showed the molecular structure of $(C_{14}H_{29})_2$ -[7]phenacene, as well as the closed molecular stacking indicative of a strong fastener effect between alkyl chains. The X-ray diffraction pattern of thin films of $(C_{14}H_{29})_2$ -[7]phenacene formed on an SiO₂/Si substrate suggested that the molecule stood on the surface with an inclined angle of 30° with respect to the normal axis of the surface. The FET properties were recorded in two-terminal measurement mode, showing p-channel normally-off characteristics. The averaged values of field-effect mobility, μ , were 1.6(3) cm² V⁻¹ s⁻¹ for a $(C_{14}H_{29})_2$ -[7]phenacene thin-film FET with SiO₂ gate dielectric and 6(4) $\times 10^{-1}$ cm² V⁻¹ s⁻¹ for a $(C_{14}H_{29})_2$ -[7]phenacene thin-film EDL FET with bmim[PF₆]. Thus, higher FET performance was obtained with an FET using a thin film of $(C_{14}H_{29})_2$ -[7]phenacene compared to parent [7]phenacene. This study could pioneer an avenue for the realization of high-performance FETs through the addition of alkyl chains to phenacene molecules.

1. Introduction

Polycyclic aromatic compounds are of great importance in materials science, particularly as promising semiconductors for organic electronics such as field-effect transistors (FETs), photovoltaics, and light-emitting devices.¹⁻⁵ The replacement of conventional silicon-based semiconductors with organic ones could be the key for future ubiquitous electronic devices, enabling light weight, flexibility, large-area coverage, ease of design, and low energy-consumption in production, to achieve the sustainable development goals (SDGs) adopted by the United Nations (UN). Various organic FET devices have been developed during the last forty years, with new materials synthesized for active-layer use, and the value of the field-effect mobility, μ , has increased due to improved fabrication processes, as well as the creation of suitable organic semiconductors. Actually, the μ value of an FET device with a polythiénylenevinylene thin film reported in 1993 was at most $\mu = 0.22 \text{ cm}^2 \text{ V}^{-1} \text{ s}^{-1}$.⁶

It is well known that the pentacene molecule forms one of the functional active layers in thin-film organic FETs. Since confirmation of the high FET utility of pentacene,⁷ there has been extensive development of FET devices using thin films of pentacene and its related compounds for more than two decades.⁸ Pentacene-based thin-film FET devices displayed μ values of $1.5\text{--}5 \text{ cm}^2 \text{ V}^{-1} \text{ s}^{-1}$,^{9,10} while pentacene single-crystal FETs exhibited μ values as high as $2.2 \text{ cm}^2 \text{ V}^{-1} \text{ s}^{-1}$.¹¹ It is worth noting that μ values in single-crystal FETs using acenes are in the range $10^{-2} \text{--} 4.3 \text{ cm}^2 \text{ V}^{-1} \text{ s}^{-1}$, including $0.02 \text{ cm}^2 \text{ V}^{-1} \text{ s}^{-1}$ for anthracene,¹² $0.4 \text{ cm}^2 \text{ V}^{-1} \text{ s}^{-1}$ for tetracene,¹³ $2.2 \text{ cm}^2 \text{ V}^{-1} \text{ s}^{-1}$ for pentacene,¹¹ and $4.3 \text{ cm}^2 \text{ V}^{-1} \text{ s}^{-1}$ for hexacene,¹⁴ indicating a straightforward increase in μ with the number (n) of benzene rings. Moreover, n-channel operation of FETs using organic molecules have also been extensively investigated,¹⁵ but a realization of high-performance n-channel FETs

was a little difficult because of an easy trap of electrons by the OH or H₂O on the surface of gate dielectric. Currently, a high n-channel FET operation ($\mu = 2.6 \text{ cm}^2 \text{ V}^{-1} \text{ s}^{-1}$) is also achieved using organic polymer material.¹⁶

As for small-molecule n-channel organic materials, rylene diimides typified by naphthalene and perylene diimides have extensively been investigated and developing new derivatives are still being continued.¹⁷ Recently, *N*-heteroarenes have attract much interest as n-channel materials due to high electron mobility.¹⁸ Benzodifurandione-oligo- (*p*-phenylenevinylene) (BDOPV) derivatives served as an active layer in high-performance n-channel FETs to display the highest μ value exceeding $10 \text{ cm}^2 \text{ V}^{-1} \text{ s}^{-1}$.¹⁹ Such n-channel materials are desired to make fully organic logic operators like complementary metal-oxide (CMOS) circuits.²⁰

The phenacene molecule is an acene isomer with zigzag-fused benzene rings. Unlike many acenes, phenacene molecules are quite stable when exposed to light and molecular oxygen. Although they have been investigated less than other acenes, we demonstrated a high potential utility of the picene molecule ([5]phenacene) in the active layer of an FET device for the first time.²¹ Since this discovery, new phenacene molecules have been synthesized, and their utility in FET devices has been examined.²¹⁻³⁰ It has been shown that [n]phenacene ($n = 5 - 11$) can effectively serve as the active layer in FET devices, with the μ value reaching $2.7 - 3.9 \text{ cm}^2 \text{ V}^{-1} \text{ s}^{-1}$ in a [6]phenacene thin-film FET;²⁴ the best μ value was $7.4 \text{ cm}^2 \text{ V}^{-1} \text{ s}^{-1}$.²⁴ Also n-channel operation was realized for the [6]phenacene thin-film FET by using Sr electrodes.²⁴ Moreover, low-voltage operation in a phenacene FET has been achieved using high-*k* gate dielectrics.²³⁻³¹ Complementary MOS (CMOS) logic circuits have also been fabricated based on the outstanding FET performance of phenacene molecules.³² Single-crystal EFT devices using [n]phenacene

($n = 5 - 9$) displayed very high μ values of $0.47 - 10.5 \text{ cm}^2 \text{ V}^{-1} \text{ s}^{-1}$ when used in SiO_2 gate dielectrics,^{27,29,33-35} and reached $17.9 \text{ cm}^2 \text{ V}^{-1} \text{ s}^{-1}$ in a [9]phenacene single-crystal FET with a ZrO_2 gate dielectric.²⁹ The μ value increased linearly with increasing n . Examination of a series of phenacene molecules in FETs showed that an extension of the π -conjugation network would enhance the μ value.²⁹

Chemical modification of π -conjugated organic molecules with long alkyl chains is one of the strategies to enhance their utility in FETs by improving their molecular packing in thin films and single crystals,³⁶ and has been successfully applied to [1]benzothieno[3,2-*b*][1]benzothiophene (BTBT) and related compounds.³⁷ For example, the μ value of an FET with dioctyl-substituted BTBT (C8-BTBT) was reported to be $1.80 \text{ cm}^2 \text{ V}^{-1} \text{ s}^{-1}$,³⁸ and through improved thin-film fabrication it reached $43 \text{ cm}^2 \text{ V}^{-1} \text{ s}^{-1}$.³⁹ Moreover, the addition of alkyl chains in picene and [6]phenacene along the long-axis direction (Fig. 1) has been performed due to the expectation of close packing by the fastener effect.^{40,41} Also, the μ value of thin film FET with $(\text{C}_{14}\text{H}_{29})_2$ -picene reached $21 \text{ cm}^2 \text{ V}^{-1} \text{ s}^{-1}$ when using a $\text{PbZr}_{0.52}\text{Ti}_{0.48}\text{O}_3$ (PZT) gate dielectric, which is one of the highest μ values evaluated from the transfer curves measured in two-terminal measurement mode.⁴⁰ The μ value is much higher than that for the parent picene molecule without alkyl chains.^{21,22} Thus, the chemical modification of the phenacene framework with alkyl chains is an effective way to enhance their FET performance.

As a consequence, we propose that both the extension of the π -conjugation network (i.e. an increment in the number of benzene rings) and the addition of alkyl chains would enhance the μ value in the thin film FET. With this in mind, the alkyl-substituted [7]phenacene, $(\text{C}_{14}\text{H}_{29})_2$ -[7]phenacene (Fig. 1), was synthesized and applied to the active layer of an FET device. This study will lead to a deeper insight into the effects on FET

characteristics brought about by the addition of alkyl chains for the π -extended phenacene molecules. Also, the utility of the newly developed alkyl-substituted phenacene molecule in an electric double layer (EDL) FET device was examined in this study. Throughout this paper, the synthesis protocol and characterization of $(C_{14}H_{29})_2$ -[7]phenacene are fully reported, and the FET performance of a $(C_{14}H_{29})_2$ -[7]phenacene thin film FET is clarified and discussed to obtain some clues leading to the realization of high performance practical FETs using phenacene molecules.

2. Experimental

2-1. Materials

Details of the preparation and physical data for the synthesized compounds are deposited in Electronic Supplementary Information (ESI, Figs. S1–S13).

2-2. XRD, UV-vis, PYS and AFM measurements of $(C_{14}H_{29})_2$ -[7]phenacene

The X-ray diffraction (XRD) pattern of a polycrystalline $(C_{14}H_{29})_2$ -[7]phenacene sample was measured with $CuK\alpha$ radiation (wavelength $\lambda = 1.5418 \text{ \AA}$) using a RIGAKU SMARTLAB-PRO; the measurement temperature was room temperature, and the sample was introduced into a capillary for XRD measurement. The Le Bail analysis was made using the GSAS program.⁴² The XRD pattern of a thin film of $(C_{14}H_{29})_2$ -[7]phenacene was measured at room temperature using the same equipment as that described above. For the XRD measurement, a 60 nm thin-film of $(C_{14}H_{29})_2$ -[7]phenacene was formed on the SiO_2 / Si substrate by thermal deposition under 10^{-7} Torr.

The UV-visible (UV-vis) absorption spectrum of a $(C_{14}H_{29})_2$ -[7]phenacene thin-film was measured at room temperature using a UV-vis spectrometer (JASCO V-670 iRM

EX). For the measurement of UV-vis spectrum, a 60 nm film of $(C_{14}H_{29})_2$ -[7]phenacene was formed on a quartz substrate by thermal deposition under 10^{-7} Torr. Photoelectron yield spectroscopy (PYS) of the film of $(C_{14}H_{29})_2$ -[7]phenacene was measured at room temperature using a PYS spectrometer (Bunko-keiki BIP-KV201). For the measurement of the PYS spectrum, a 60 nm film of $(C_{14}H_{29})_2$ -[7]phenacene was formed on an SiO_2 / Si substrate. During the thermal deposition of $(C_{14}H_{29})_2$ -[7]phenacene, both substrates were kept at $120^\circ C$. Atomic force microscope (AFM) images of thin films of $(C_{14}H_{29})_2$ -[7]phenacene formed on SiO_2 and ZrO_2 were measured by use of an AFM measurement system (SII Nano Technology SPA400) at room temperature.

2-3. STM and STS of $(C_{14}H_{29})_2$ -[7]phenacene adsorbed on Au(111)

Scanning tunneling microscopy (STM) and spectroscopy (STS) experiments were performed at 77 K under pressure of $\sim 10^{-10}$ Torr with a Pt / Ir tip. A well-defined Au(111) surface was prepared by Ar ion sputtering and annealing. The sample of $(C_{14}H_{29})_2$ -[7]phenacene was deposited in-situ onto the room-temperature Au(111) substrate at a rate of 0.03 – 0.1 ML / min from the crucible heated at $145 - 152^\circ C$.

2-4. Preliminary treatment of SiO_2 / Si and ZrO_2 / Si substrates

The commercially available SiO_2 / Si substrate was cleaned according to the procedure described elsewhere.³² After the cleaning of the substrate, the surface of SiO_2 / Si substrate was treated with a mixed solution of hexamethyldisilazane (HMDS) and hexane (volume ratio of 1 : 9) for a half day to form the hydrophobic surface. The substrate was finally washed with methanol and then with ultra-purified water under

ultrasonic irradiation, each for 5 min. The substrate was dried under a N₂ gas flow, and it was heated at 105°C for 3 min.

The commercially available ZrO₂ / Si substrate was washed with isopropanol and then with ultra-purified water under ultrasonic irradiation, each for 5 min; the ZrO₂ film was formed on Si substrate by RF sputter deposition. The substrate was finally dried by spraying N₂ gas. The ZrO₂ / Si substrate was covered with 50 nm thick parylene to make the hydrophobic surface and avoid the leakage of gate current; the parylene coating was made by thermal deposition of parylene-C under Ar atmosphere. Details of preparation of parylene film is described in ref. 43.

2-5. Fabrication of (C₁₄H₂₉)₂-[7]phenacene thin-film FET devices and measurement of FET characteristics

A 60 nm thick thin-film of (C₁₄H₂₉)₂-[7]phenacene was formed for an active layer on solid gate dielectrics of SiO₂ and ZrO₂ by the thermal deposition of (C₁₄H₂₉)₂-[7]phenacene under a vacuum of 10⁻⁷ Torr; thickness of SiO₂ was 400 nm, while that of ZrO₂ was 150 nm which was covered with 50 nm thick parylene. The SiO₂ / Si and ZrO₂ / Si substrates were heated at 120°C during the thermal deposition of (C₁₄H₂₉)₂-[7]phenacene for the formation of the active layer. The shape of the thin films was determined by use of a metal mask. Three nm thick 2,3,5,6-tetrafluoro-7,7,8,8-teracyanoquinodimethane (F4TCNQ) was deposited on the (C₁₄H₂₉)₂-[7]phenacene thin film, and the source and drain electrodes were formed by the thermal deposition of Au on the F4TCNQ. Thus, the F4TCNQ layer was inserted between the Au source / drain electrodes and the (C₁₄H₂₉)₂-[7]phenacene thin film so as to reduce contact resistance. The device structure (top contact / bottom gate FET device) is shown in Fig. 2(a).

All measurements were made in two-terminal measurement mode at room temperature with an Agilent B1500A semiconductor parametric analyzer; the FET characteristics in FET devices with solid gate dielectrics were measured under a vacuum of 10^{-8} Torr. The measured transfer curves were analyzed to determine the FET parameters (μ , threshold voltage (V_{th}), on/off ratio and subthreshold swing (S)) using the general formula for a saturation regime:

$$I_D = \frac{\mu W C_o}{2L} (V_G - V_{th})^2 \quad (1)$$

where I_D , V_G , V_{th} , W , L and C_o refer to drain current, gate voltage, threshold voltage, channel width, channel length and capacitance per area of gate dielectric, respectively; the value of drain voltage, V_D , is fixed in the measurement of the transfer curve. The capacitance, C_o , was determined by extrapolation of the capacitance recorded at 20 Hz – 1000 Hz to 0 Hz with an AC amplitude of 1.0 V using LCR meter (Agilent E4980A), and detailed value of C_o for each gate dielectric is described later. The condition for a saturation regime, $V_D > V_G - V_{th}$, was completely satisfied in the analysis of the transfer curve; in p-channel measurement mode, absolute values of V_D , V_G and V_{th} are employed for the analysis. Saturation is observed in the output characteristics of all FETs. All FET parameters were evaluated from the forward transfer curve, in case of no comment.

2-6. Fabrication of a $(C_{14}H_{29})_2$ -[7]phenacene EDL thin-film FET device and measurement of FET characteristics

The $(C_{14}H_{29})_2$ -[7]phenacene EDL thin-film FET was prepared by using an ionic liquid for the gate dielectric, where the ionic liquid was 1-butyl-3-methylimidazolium hexafluorophosphate (bmim[PF₆]). The bmim[PF₆] was levigated to make the ionic liquid (bmim[PF₆]) polymer sheet by adding poly(styrene-*b*-ethylene oxide-*b*-styrene), and was

placed across the side gate electrode and $(C_{14}H_{29})_2$ -[7]phenacene thin film. The thin film of $(C_{14}H_{29})_2$ -[7]phenacene was formed as the active layer on a SiO_2 / Si substrate, and 50 nm thick Au source and drain electrodes were formed on the above thin film. F4TCNQ was also inserted between the Au source / drain electrodes and the $(C_{14}H_{29})_2$ -[7]phenacene thin film. In the same manner as when forming the active layer in the $(C_{14}H_{29})_2$ -[7]phenacene thin-film FET with solid gate dielectrics (section 2-5), the above substrate was heated at 120°C during the thermal deposition. The gate voltage was applied for the bmim[PF₆] polymer sheet from the side-gate electrode. Thus, the EDL FET device has a top contact / side-gate type structure, as seen from Fig. 2(b). The FET characteristics of the EDL FET device set in an Ar-filled glove box were measured using the same method as that described in section 2-5.

3. Results

3-1. Synthesis and characterization of $(C_{14}H_{29})_2$ -[7]phenacene

The phenacene molecules were constructed by various synthetic procedures.⁴⁴⁻⁴⁶ One of the most reliable and common methods is the Mallory photoreaction, by which 1,2-diarylethene precursors can be effectively converted into the corresponding phenacene frameworks via 6π -photocyclization, followed by oxidative aromatization in the presence of oxygen and iodine.⁴⁴ We have also synthesized various phenacene derivatives including $(C_{14}H_{29})_2$ -picene by photoreaction.^{28-30,40} It is reasonable to expect that the π -extended homologue, $(C_{14}H_{29})_2$ -[7]phenacene, can be synthesized via the Mallory photoreaction.

The synthetic route to $(C_{14}H_{29})_2$ -[7]phenacene is illustrated in Scheme 1. The structures of the new compounds were assigned by NMR, IR, and elemental analysis, or

high-resolution mass spectrometry. The detailed experimental procedures and physical data of the new compounds are deposited in ESI.

Starting compound **1** was successively treated with BuLi and DMF to afford aldehyde **2**. Compound **2** was converted to triflate **4** through deprotection by tetrabutylammonium fluoride (TBAF), reaction with triflic anhydride (Tf₂O), and protection of the formyl group as acetal. Tetradecyl side chains were efficiently introduced as compound **6** by a Sonogashira reaction using Pd(PPh₃)₂Cl₂ and CuI as catalysts in *i*-Pr₂NH. The triple bonds of compound **5** were hydrogenated under H₂/PtO₂ to form compound **6**. Then acetal was removed by acidic hydrolysis to form tetradecyl-substituted aldehyde **7** as one of the Wittig coupling components. Compound **7** was reduced with NaBH₄ to afford alcohol **8** which was reacted with PBr₃ to form compound **9**. Compound **9** was reacted with PPh₃ to form phosphonium salt **10**. Compound **10** was obtained as an oily material and used in the following reaction without purification. The Wittig reaction between aldehyde **7** and phosphonium salt **10** was conducted by using tetrabutylammonium hydroxide (TBAOH) as a base to form dialylethene **11**, which was the precursor to the target compound. From ¹H NMR spectral analysis, dialylethene **11** was assignable to a ca. 1:1 mixture of *E* and *Z* isomers (Fig. S13 in ESI).

The mixture was subjected to Mallory photocyclization without separating the isomers. Thus, a refluxing solution of dialylethene **11** in chlorobenzene was irradiated with black-light lamps (365 nm) in the presence of I₂ under aerated conditions to obtain (C₁₄H₂₉)₂-[7]phenacene as an off-white precipitate. The Mallory photocyclization step is advantageous because the final product was obtained only by collecting the precipitate and no further separation/purification was needed. Additionally, because solubility of [7]phenacene derivatives is quite poor in common organic solvents, introducing

appropriate functionalities directly into [7]phenacene core is unfavorable. Therefore, construction of the [7]phenacene skeleton in the final step is critical to achieve synthesis of the chemically modified [7]phenacene.

The structure of $(C_{14}H_{29})_2$ -[7]phenacene was assigned by comparing its 1H NMR spectral data with that for parent [7]phenacene. Fig. 3 shows 1H NMR spectra (aromatic region) of the two compounds. (Entire spectrum of $(C_{14}H_{29})_2$ -[7]phenacene is shown in Fig. S1 in ESI). Both compounds indicate similar spectral patterns, *i.e.*, protons located at the bay region show signals at lower field (8.8–9.2 ppm), whereas those at the edge of the molecule display signals in higher field (7.6–8.2 ppm). The signal of H_g in $(C_{14}H_{29})_2$ -[7]phenacene appeared as a singlet at 7.85 ppm. This observation provides evidence for the presence of the alkyl substituents at 3 and 12 positions. Fig. 4 shows UV-vis absorption and fluorescence emission spectra of $(C_{14}H_{29})_2$ -[7]phenacene and [7]phenacene in $CHCl_3$. Both compounds show similar spectra; a very weak absorption band at 390 nm (1L_b) and the second band at 345 nm with moderate intensity (1L_a) were observed. Additionally, the fluorescence spectrum of $(C_{14}H_{29})_2$ -[7]phenacene is essentially the same as that of the parent compound. Therefore, the C_{14} -alkyl chains have a minimal effect on the electronic features of the [7]phenacene core in solution.

3-2. Structural characterization and electronic structures of $(C_{14}H_{29})_2$ -[7]phenacene thin film on SiO_2 / Si substrate

The powder XRD pattern of a $(C_{14}H_{29})_2$ -[7]phenacene sample is shown in Fig. 5(a), together with the pattern calculated by Le Bail analysis. The XRD pattern was analyzed under the space group of $P2_1$ (monoclinic lattice (No. 4)), and the lattice constants, a , b , c and β were determined to be 13.1749(4) Å, 5.5116(5) Å, 45.216(3) Å and 95.230(4)°,

respectively, by Le Bail analysis. The calculated pattern fits the experimental XRD pattern well, showing that the pattern R factor, R_p , and weighted pattern R factor, wR_p , are 3.62% and 4.55%, respectively. For the comparison, the lattice constants of $(C_{14}H_{29})_2$ -[7]phenacene and [7]phenacene are listed in Table 1. The c value is much larger than that, 17.829(2) Å, of [7]phenacene,⁴⁷ as seen from Table 1, indicating that the long axis is substantially directed along the c axis.

The XRD pattern of $(C_{14}H_{29})_2$ -[7]phenacene thin film is shown in Fig. 5(b), which shows only $00l$ peaks, indicating that the $(C_{14}H_{29})_2$ -[7]phenacene molecules are well aligned along the axis perpendicular to the ab plane, which corresponds to reciprocal lattice c , c^* . Here, it should be noticed that the SiO_2 / Si substrate was heated at 120°C during the formation of the $(C_{14}H_{29})_2$ -[7]phenacene thin film. Actually, no peaks were observed when the $(C_{14}H_{29})_2$ -[7]phenacene thin film was formed without heating the substrate. The value of $1/|c^*|$ was determined to be 45(1) Å from three peaks (001, 002 and 003). Thus, the $1/|c^*|$ value is the same as the c value, 45.216(3) Å, of the polycrystalline powder sample, indicating $\beta \approx 90^\circ$. Actually, the β was 95.230(4)°. The tilted angle, θ , of the long axis of $(C_{14}H_{29})_2$ -[7]phenacene molecule with respect to the c^* axis was estimated to be 30° (see Fig. 5(c)), because the calculated long axis of a $(C_{14}H_{29})_2$ -[7]phenacene molecule is 51.74 Å. The θ value was consistent with that of [7]phenacene.^{29,30}

The UV-vis absorption and PYS spectra are shown in Figs. 6(a) and (b), respectively. The onset energy in the UV-vis spectrum is 3.0 eV, which refers to the energy difference between the highest occupied molecular orbital (HOMO) and the lowest unoccupied molecular orbital (LUMO). The onset energy in the PYS spectrum is 5.7 eV, which indicates a HOMO level of -5.7 eV. The results imply the presence of a HOMO at -5.7

eV and a LUMO at -2.7 eV. A schematic representation of energy levels (HOMO, LUMO and energy gap) of $(C_{14}H_{29})_2$ -[5]phenacene ($(C_{14}H_{29})_2$ -picene), $(C_{14}H_{29})_2$ -[6]phenacene, $(C_{14}H_{29})_2$ -[7]phenacene and [7]phenacene is shown in Fig. 6(c), indicating that all the molecules possess almost the same energy levels. Thus the electronic state does not vary with an increase in the number of benzene rings, and the alkyl chains do not affect the substantial electronic state because the π -framework in a phenacene molecule dominates the HOMO and LUMO levels. The p-channel operation is predicted in all molecules shown in Fig. 6(c) from their characteristic electronic structures, *i.e.*, the high LUMO level must make n-channel operation impossible. Moreover, the large energy gap should provide a clear ability of on-off switch in FETs.

3-3. Characterization of $(C_{14}H_{29})_2$ -[7]phenacene thin-film on Au substrate

Fig. 7(a) shows an STM image of a full layer $(C_{14}H_{29})_2$ -[7]phenacene on a Au(111) substrate, measured at a low bias voltage of -50 mV; all benzene rings of the [7]phenacene cores and the alkyl chains are clearly observed. Self-organized growth of $(C_{14}H_{29})_2$ -[7]phenacene on Au(111) starts with submonolayer coverage, and the molecules form regular unit cells with a basis of two unequally aligned molecules, A and B, shown in Fig. 7(a), with the alkyl chains alternately stacked. These results suggest the presence of a strong fastener effect between alkyl chains in $(C_{14}H_{29})_2$ -[7]phenacene molecules on the Au surface.

An adsorption of the molecular plane parallel to the surface is observed due to a strong molecule-substrate interaction. As seen from the inset of Fig. 7(a), the intramolecular contrast is enhanced at an elevated bias voltage of -2.5 V, where electrons tunnel directly into molecular states. Within an angular variation of $\pm 3^\circ$, alkyl chains are

aligned parallel to neighboring molecules. Depending on the observed areas (Structure 1, Structure 2 and Structure 3), a small variation of the unit cell is found, as seen from the parameters given in Table 2.

The STS spectra are shown in Fig. 7(b). As seen from Fig. 7(b), a dominant contribution of the electron density is due to the [7]phenacene core, and the HOMO and LUMO states are observed with a band gap of ~ 3.05 eV. In addition, a broad shoulder found in the unoccupied states below the LUMO originates from the alkyl chains. The value of the energy gap is consistent with the value, 3.0 eV, obtained from the UV-Vis absorption spectrum (Fig. 6(a)). The interaction of the molecules with the substrate will perturb the electronic structure to induce a molecule-metal hybrid state with an energetically broad band. The above energetically broad shoulder may be due to this interaction.

As seen from Fig. 7(b), the XRD pattern of a 100 nm thick thin-film of $(C_{14}H_{29})_2$ -[7]phenacene on an Au substrate includes only $00l$ peaks, indicating that the ab -plane is parallel to the Au surface. The value of $1/|c^*|$ for a 100 nm thick thin-film of $(C_{14}H_{29})_2$ -[7]phenacene on an Au substrate was $45(2)$ Å, which is the same as that ($= 45(1)$ Å) on an SiO_2 / Si substrate. This result implies that the long axis of the $(C_{14}H_{29})_2$ -[7]phenacene molecule is oriented along the direction normal to the surface of the Au substrate, which is the same as in the case of an SiO_2 / Si substrate; the result is inconsistent with the packing style of the $(C_{14}H_{29})_2$ -[7]phenacene molecules derived from the STM image (Fig. 7(a)).

As a consequence, the orientation of $(C_{14}H_{29})_2$ -[7]phenacene molecule in the first layer (*i.e.*, monolayer coverage) determined from the STM image is different from that in the 100 nm thick thin-film, indicating that the above packing style found in the monolayer

of $(C_{14}H_{29})_2$ -[7]phenacene on Au substrate must be strongly affected by an interaction between the molecule and Au(111) surface.

3-4. FET properties of $(C_{14}H_{29})_2$ -[7]phenacene thin-film FETs with SiO_2 and ZrO_2 gate dielectrics

The device structure of a $(C_{14}H_{29})_2$ -[7]phenacene thin-film FET with SiO_2 gate dielectric is shown in Fig. 2(a). Figs. 8(a) and (b) show the transfer and output curves for a $(C_{14}H_{29})_2$ -[7]phenacene thin-film FET formed on an SiO_2 / Si substrate; 400 nm thick SiO_2 was used as the gate dielectric, and the capacitance per area, C_o , was 8.34 nF cm^{-2} , as determined by the extrapolation of C_o recorded at 20–1000 Hz to 0 Hz.

The absolute drain current, $|I_D|$, increases with application of a negative gate voltage, V_G . The value of $|I_D|$ increases with an increase in $|V_G|$, in which the drain voltage V_D was fixed at -100 V . The transfer curve (Fig. 8(a)) shows p-channel operation, since the negative V_G was applied for the increase in $|I_D|$. The output curves, $|I_D| - |V_D|$ plots, at different negative V_G values provided typical normally-off properties (Fig. 8(b)), indicating that the $(C_{14}H_{29})_2$ -[7]phenacene thin-film FET exhibits p-channel normally-off FET properties. The values of μ , $|V_{th}|$, on/off ratio and S were determined to be $2.03 \text{ cm}^2 \text{ V}^{-1} \text{ s}^{-1}$, $2.49 \times 10^1 \text{ V}$, 1.5×10^6 and $2.0 \text{ V decade}^{-1}$, respectively, showing excellent p-channel normally-off FET properties. We additionally estimated the μ value from the output curves at $|V_D| = 100 \text{ V}$ (Figure 8(b)) to check the possible overestimation of the above μ value ($= 2.03 \text{ cm}^2 \text{ V}^{-1} \text{ s}^{-1}$). As a consequence, the μ value was determined to be $1.40 \text{ cm}^2 \text{ V}^{-1} \text{ s}^{-1}$. This value is a little smaller than that determined from the transfer curve, but it is still high μ value in organic thin-film FETs. Thus, the excellent p-channel properties were confirmed from both transfer and output curves.

Here, we must briefly comment on a significant hysteresis between forward and reverse transfer curves, which is presumably due to a bias stress effect produced by a trace of water on SiO₂ gate dielectric. Actually, the surface of SiO₂ was treated by HMDS to provide the hydrophobic surface, but the surface treatment by HMDS may not lead to the sufficient hydrophobic surface to disappear the hysteresis. As described later, no hysteresis was observed in case of the parylene coated ZrO₂.

Table 3 lists the FET parameters of the (C₁₄H₂₉)₂-[7]phenacene thin-film FET with an SiO₂ gate dielectric. The averaged values of μ , $|V_{th}|$, on/off ratio and S ($\langle\mu\rangle$, $\langle|V_{th}|\rangle$, $\langle\text{on/off ratio}\rangle$ and $\langle S\rangle$) were 1.6(3) cm² V⁻¹ s⁻¹, 2.2(7) × 10¹ V, 8(6) × 10⁶ and 3(2) V decade⁻¹, respectively; the averaged values were obtained from nine FET devices. Thus, the FET performance is relatively high.

For comparison, the transfer and output curves of [7]phenacene thin-film FET with SiO₂ gate dielectric are shown in Figs. 8(c) and (d), respectively, which show p-channel operation. The output curves, $|I_D| - |V_D|$ plots, at different negative V_G values provided typical normally-off properties. The values of μ , $|V_{th}|$, on/off ratio and S were determined to be 9.2 × 10⁻¹ cm² V⁻¹ s⁻¹, 6.61 × 10¹ V, 1.9 × 10⁶ and 3.74 V decade⁻¹, respectively, showing good p-channel normally-off FET properties. FET parameters of all [7]phenacene thin-film FETs measured in this study are listed in Table 4. The averaged μ value was 5(2) × 10⁻¹ cm² V⁻¹ s⁻¹ which was determined from eight devices. The μ value is similar to that, 7.5 × 10⁻¹ cm² V⁻¹ s⁻¹, for [7]phenacene thin-film FET with SiO₂ gate dielectric reported previously.²⁵ Therefore, the μ value of (C₁₄H₂₉)₂-[7]phenacene is higher than that of pure [7]phenacene molecule. This result indicates the effectiveness of an introduction of alkyl chains to [7]phenacene, *i.e.*, the importance of fastener effect for improvement of FET properties.

The device structure of the $(C_{14}H_{29})_2$ -[7]phenacene thin-film FET with a ZrO_2 gate dielectric is shown in Fig. 2(a). Figs. 9(a) and (b) show the transfer and output curves for a $(C_{14}H_{29})_2$ -[7]phenacene thin-film FET formed on a ZrO_2 / Si substrate; 150 nm thick ZrO_2 was used as the gate dielectric, and the capacitance per area, C_o , was 38.9 nF cm^{-2} , as determined by the extrapolation of C_o recorded at 20–1000 Hz to 0 Hz.

The absolute drain current, $|I_D|$, increases with application of the negative gate voltage, V_G , in the same manner as in the $(C_{14}H_{29})_2$ -[7]phenacene thin-film FET with an SiO_2 gate dielectric. The value of $|I_D|$ increases with an increase in $|V_G|$, in which the drain voltage V_D was fixed at -18 V , showing a low-voltage operation. The transfer curve (Fig. 9(a)) shows p-channel operation, since the negative V_G increases the $|I_D|$. The output curves, $|I_D| - |V_D|$ plots at different negative V_G values, provided typical normally-off properties. The values of μ , $|V_{th}|$, on/off ratio and S were determined to be $2.15 \times 10^{-1} \text{ cm}^2 \text{ V}^{-1} \text{ s}^{-1}$, 6.4 V , 1.1×10^6 and $3.8 \times 10^{-1} \text{ V decade}^{-1}$, respectively, indicating p-channel normally-off FET properties and low-voltage operation. Table 5 lists the FET parameters of the $(C_{14}H_{29})_2$ -[7]phenacene thin-film FET with ZrO_2 gate dielectric. The $\langle \mu \rangle$, $\langle |V_{th}| \rangle$, $\langle \text{on/off ratio} \rangle$ and $\langle S \rangle$ were $1.1(5) \times 10^{-1} \text{ cm}^2 \text{ V}^{-1} \text{ s}^{-1}$, $7(2) \text{ V}$, $6(4) \times 10^5$ and $6(2) \times 10^{-1} \text{ V decade}^{-1}$, respectively; the averaged values were obtained from seven FET devices.

Here, we must comment on the relatively low μ value in $(C_{14}H_{29})_2$ -[7]phenacene thin-film FET with an ZrO_2 gate dielectric, because the μ values in phenacene FETs using high- k gate dielectric is generally higher than that in case of SiO_2 gate dielectric.^{28,30} As seen from the AFM images of $(C_{14}H_{29})_2$ -[7]phenacene thin films formed on SiO_2 and ZrO_2 (Fig. S3), the root mean square (RMS) of surface roughness of thin film on ZrO_2 ($5.0 \times 10^1 \text{ nm}$) was larger by one order of magnitude than that on SiO_2 (4.1 nm),

indicating that the low μ value for $(C_{14}H_{29})_2$ -[7]phenacene thin-film FET with an ZrO_2 gate dielectric probably is due to the low quality (large roughness) of thin film. The reason why the quality of thin film is low in case of ZrO_2 may be ascribed to the thermal damage of parylene with which ZrO_2 surface is coated, because the parylene-coated ZrO_2 / Si substrate was heated at 120°C during the thermal deposition of $(C_{14}H_{29})_2$ -[7]phenacene. On the other hand, it can be stressed that a hysteresis between forward and reverse transfer curves was not observed. Namely, the parylene coating of ZrO_2 surface provides the sufficient hydrophobic surface to disappear the hysteresis. As a consequence, in the next study we must keep in mind the formation of $(C_{14}H_{29})_2$ -[7]phenacene thin film with high quality on parylene-coated ZrO_2 surface for increasing the μ value, as well as decreasing the hysteresis in transfer curves.

3-5. Fabrication and characterizations of $(C_{14}H_{29})_2$ -[7]phenacene thin-film EDL FET

A $(C_{14}H_{29})_2$ -[7]phenacene thin-film FET was fabricated using a gate dielectric consisting of an ionic liquid, bmim[PF₆], as shown in Fig. 2(b); the gate dielectric is called an ‘electric double-layer (EDL) capacitor’. The C_0 is as high as 8.01 $\mu\text{F cm}^{-2}$, which is higher by three orders of magnitude than that with an SiO_2 gate dielectric. Figs. 10(a) and (b) show the transfer and output characteristics for a $(C_{14}H_{29})_2$ -[7]phenacene thin-film EDL FET. The $|I_D|$ increases with application of a negative V_G , indicating p -channel operation and very low-voltage operation, *i.e.*, $|I_D|$ increased with increasing $|V_G|$, when V_D was fixed at -1.0 V. The transfer curves show very large hysteresis, *i.e.*, the reverse $|I_D| - |V_G|$ is significantly different from that of the forward $|I_D| - |V_G|$ plot. The $|I_D| - |V_D|$ plots at different negative V_G values exhibited normally-off properties.

The values of μ , $|V_{th}|$, on/off ratio and S were determined to be $1.25 \text{ cm}^2 \text{ V}^{-1} \text{ s}^{-1}$, 2.40 V , 2.2×10^2 and $2.99 \times 10^{-1} \text{ V decade}^{-1}$, respectively, from the forward transfer curve. Thus, the FET characteristics of a $(\text{C}_{14}\text{H}_{29})_2$ -[7]phenacene thin-film EDL FET are summarized as ‘high field-effect mobility and extremely low threshold voltage’. Actually, the hysteresis in forward and reverse transfer curves is very large in the EDL FET, leading to the different FET properties between forward and reverse transfer curves. To avoid the overestimation of the FET properties, the values of μ , $|V_{th}|$, on/off ratio and S were also evaluated from the reverse transfer curve, which provided the values of $3.21 \times 10^{-1} \text{ cm}^2 \text{ V}^{-1} \text{ s}^{-1}$, 1.93 V , 1.9×10^2 and $8.76 \times 10^{-2} \text{ V decade}^{-1}$, respectively.

Table 6 lists the FET parameters of six $(\text{C}_{14}\text{H}_{29})_2$ -[7]phenacene EDL thin-film FETs, which were determined from both the forward and reverse transfer curves. The $\langle\mu\rangle$, $\langle|V_{th}|\rangle$, $\langle\text{on/off ratio}\rangle$ and $\langle S\rangle$ were $1.0(2) \text{ cm}^2 \text{ V}^{-1} \text{ s}^{-1}$, $2.3(2) \text{ V}$, $6(5) \times 10^3$ and $2.1(9) \times 10^{-1} \text{ V decade}^{-1}$, respectively, for the forward transfer curve, while they were $2.7(6) \times 10^{-1} \text{ cm}^2 \text{ V}^{-1} \text{ s}^{-1}$, $1.9(1) \text{ V}$, $3(1) \times 10^2$ and $3(2) \times 10^{-1} \text{ V decade}^{-1}$ for the reverse transfer curves. The averaged values of $\langle\mu\rangle$, $\langle|V_{th}|\rangle$, $\langle\text{on/off ratio}\rangle$ and $\langle S\rangle$ between forward and reverse transfer curves were $6(4) \times 10^{-1} \text{ cm}^2 \text{ V}^{-1} \text{ s}^{-1}$, $2.1(3) \text{ V}$, $3(4) \times 10^2$ and $3(1) \times 10^{-1} \text{ V decade}^{-1}$; the averaged values reflect FET properties without overestimation. The averaged μ value of $6(4) \times 10^{-1} \text{ cm}^2 \text{ V}^{-1} \text{ s}^{-1}$ is relatively high, and the $\langle V_{th}\rangle$ value of $2.1(3) \text{ V}$ is sufficiently low. Thus, it was found that the $(\text{C}_{14}\text{H}_{29})_2$ -[7]phenacene molecule was available for an EDL thin-film FET.

4. Discussion

The FET properties of alkyl-substituted phenacene have been investigated using $(\text{C}_{14}\text{H}_{29})_2$ -picene and $(\text{C}_{14}\text{H}_{29})_2$ -[6]phenacene.^{40,41} FET devices using a thin film of

(C₁₄H₂₉)₂-picene showed quite excellent FET properties, *i.e.*, the μ value of $\sim 21 \text{ cm}^2 \text{ V}^{-1} \text{ s}^{-1}$ was achieved with a (C₁₄H₂₉)₂-picene thin-film FET with an SiO₂ gate dielectric. The μ value is higher by one order of magnitude than that ($\sim 3 \text{ cm}^2 \text{ V}^{-1} \text{ s}^{-1}$) of an FET with a thin film of picene without alkyl substituents,^{21,22} indicating the significance of the fastener effect of alkyl chains on the close packing between molecules. Moreover, a drastic increase in μ value against the number (n) of benzene rings in a phenacene molecule has been evidenced in the FETs with single crystals of picene up to [9]phenacene (n = 5 – 9),²⁹ *i.e.*, a more extended π -network in the molecule provides closer packing to show a higher μ value, as described in the Introduction. Thus the improvement of FET properties has been effected through a combination of the fastener effect and the extension of the π -network.

In fact, the usage of a thin film of (C₁₄H₂₉)₂-[7]phenacene in an FET device led to an averaged μ value as high as $10^{-1} - 1.6 \text{ cm}^2 \text{ V}^{-1} \text{ s}^{-1}$, which is lower by one order of magnitude than that from using (C₁₄H₂₉)₂-picene,⁴⁰ although the above μ value is not so bad. The STM image for the monolayer of (C₁₄H₂₉)₂-[7]phenacene showed the close packing between molecules through a strong fastener effect (Fig. 7(a)), but the packing form was quite different from that of a thin film, *i.e.*, the framework of (C₁₄H₂₉)₂-[7]phenacene was oriented in parallel to the substrate, which is not effective for electric transport in the FET device. The above orientation of (C₁₄H₂₉)₂-[7]phenacene in the first layer on the substrate may provide a lower μ value than that in (C₁₄H₂₉)₂-picene FET because the first layer forms the channel region in FET. However, the above scenario is still under discussion since the information of the packing form of the (C₁₄H₂₉)₂-picene in the channel region has not been obtained. In addition, the $\langle \mu \rangle$ value, $1.6(3) \text{ cm}^2 \text{ V}^{-1} \text{ s}^{-1}$, of (C₁₄H₂₉)₂-[7]phenacene with SiO₂ gate dielectric (Table 3) was higher than the $\langle \mu \rangle$

value of $5(2) \times 10^{-1} \text{ cm}^2 \text{ V}^{-1} \text{ s}^{-1}$ for [7]phenacene thin-film FET obtained in this study (Table 4), and the previously reported μ value, $7.5 \times 10^{-1} \text{ cm}^2 \text{ V}^{-1} \text{ s}^{-1}$, for [7]phenacene thin-film FET.²⁵ Namely, the effect of addition of alkyl substituents on FET performance is partially found, although it is not so clear in comparison with case of picene. Therefore, we suggest the importance of fastener effect for the improvement of FET properties.

The type of the alkyl chain must also be sufficiently discussed for realizing the drastic improvement of the μ value, as in the case of picene. In this study, we added the same alkyl chain (tetradecyl group) as the case of picene for the [7]phenacene framework because of the drastic enhancement of μ value in a $(\text{C}_{14}\text{H}_{29})_2$ -picene thin-film FET. However, it is unclear if the tetradecyl group is suitable for [7]phenacene. Since a more extended π -framework in [7]phenacene than picene would strengthen the π - π interaction between molecules, an alkyl chain with a different length than a tetradecyl group may be indispensable for [7]phenacene.

Finally, we must point out the possibility that the thin film of $(\text{C}_{14}\text{H}_{29})_2$ -[7]phenacene was not formed in the optimal condition. Here, it should be noted that the substrate was heated at 120°C during the thermal deposition of $(\text{C}_{14}\text{H}_{29})_2$ -[7]phenacene, as described in the experimental section. In fact, the FET device with a thin film of $(\text{C}_{14}\text{H}_{29})_2$ -[7]phenacene formed without heating the substrate did not operate, which means that the quality of thin film strongly depends on the condition of fabrication. Thus, the conditions forming the thin film of $(\text{C}_{14}\text{H}_{29})_2$ -[7]phenacene are more critical than in the case of $(\text{C}_{14}\text{H}_{29})_2$ -picene. Thus we may not have found the optimal conditions for formation of the active layer in a $(\text{C}_{14}\text{H}_{29})_2$ -[7]phenacene thin-film FET. Further experimental study is required for the remarkable improvement of the FET properties of a $(\text{C}_{14}\text{H}_{29})_2$ -[7]phenacene thin-film FET.

Conclusion

Ditradecyl-substituted π -extended phenacene, $(C_{14}H_{29})_2$ -[7]phenacene, was successfully synthesized using Mallory photocyclization as the key step. To the best of our knowledge, this is the first [7]phenacene derivative incorporating alkyl chains at the long axis positions of the phenacene framework. The molecular structure was confirmed by 1H NMR spectroscopy and high-resolution mass spectrometry, and the solid state structure was determined by XRD and STM imaging. The STM indicated that the $(C_{14}H_{29})_2$ -[7]phenacene molecules were deposited on the Au(111) surface and were then aggregated by the π -CH interactions between the aromatic core and the alkyl moieties. In contrast, in thin films on an SiO_2 / Si substrate, the molecules stood with the inclined angle of 30° to retain aromatic π - π interactions. The latter alignment is suitable for FET operation. The $(C_{14}H_{29})_2$ -[7]phenacene thin-film FET devices recorded averaged μ values as high as $10^{-1} - 1.6 \text{ cm}^2 \text{ V}^{-1} \text{ s}^{-1}$, which is similar to that of amorphous silicon. Also, a $(C_{14}H_{29})_2$ -[7]phenacene thin-film EDL FET device with bmim[PF₆] displayed p-channel operation with an averaged μ value of $6(4) \times 10^{-1} \text{ cm}^2 \text{ V}^{-1} \text{ s}^{-1}$. Further optimization of the FET device with $(C_{14}H_{29})_2$ -[7]phenacene is currently underway to achieve much higher FET performance. The facile synthesis of the chemically modified π -extended phenacenes will enable the development of a promising FET material for ultra-high performance organic FETs.

Electronic Supplementary Information

Details of synthetic procedures, physical data and NMR spectra of the new compounds

Conflict of Interests

There are no conflicts to declare.

Acknowledgements

This study was partly supported by Grants-in-Aid (26105004, 17K05976, 17K05500, 18K04940, 18K18736 and 19H02676) from MEXT, and the JST-ACT-C project of the Japan Science and Technology Agency (No. JPMJCR 12YW), and by the Program for Promoting the Enhancement of Research Universities from MEXT, Japan. Moreover, a part of this study (STM and STS studies) was supported by Grants (105-2112-M-007-022-MY3 and 106-2923-M-007-001-MY4) from the Ministry of Science and Technology (MOST) in Taiwan, and by the Center for Quantum Technology, National Tsing Hua University, from the Featured Areas Research Center Program within the framework of the Higher Education Sprout Project by the Ministry of Education (MOE) in Taiwan. Instrumental analyses of the novel compounds were supported by the Cooperative Research Program of the ‘Network Joint Research Center for Materials and Devices’ from MEXT, Japan. HO thanks Prof. Hiroko Yamada (NAIST) for HRMS measurement of $(C_{14}H_{29})_2$ -[7]phenacene.

References

- 1 Y. Yu, Q. Ma, H. Ling, W. Li, R. Ju, L. Bian, N. Shi, Y. Qian, M. Yi, L. Xie, and W. Huang, *Adv. Funct. Mater.*, 2019, **29**, 1904602.
- 2 C. Wang, H. Dong, L. Jiang, and W. Hu, *Chem. Soc. Rev.*, 2018, **47**, 422–500.
- 3 Y. Xu, C. Liu, D. Khim, and Y.-Y Noh, *Phys. Chem. Chem. Phys.*, 2015, **17**, 26553–26574.
- 4 J. Mei and Y. Diao, *J. Am. Chem. Soc.*, 2013, **135**, 6724–6746.
- 5 C. Wang, H. Dong, L. Jiang and W. Hu, *Chem. Soc. Rev.*, 2018, **47**, 422–500.
- 6 H. Fuchigami, A. Tsumura and H. Koezuka, *Appl. Phys. Lett.*, 1993, **63**, 1372–1374.
- 7 D. J. Gundlach, Y.-Y. Lin, T. N. Jackson, S. F. Nelson and D. G. Schlom, *IEEE Electron Device Lett.*, 1997, **18**, 87–89.
- 8 J. E. Anthony, *Chem. Rev.*, 2006, **106**, 5028–5048.
- 9 M. Shtein, J. Maple and J. B. Benziger, *Appl. Phys. Lett.*, 2002, **81**, 268–270.
- 10 T. W. Kelley, D. V. Muyres, P. F. Baude, T. P. Smith and T. D. Jones, *Mater. Res. Soc. Proc.*, 2003, **771**, 169–179.
- 11 L. B. Roberson, J. Kowalik, L. M. Tolbert, C. Kloc, R. Zeis, X. Chi, R. Fleming and C. Wilkins, *J. Am. Chem. Soc.*, 2005, **127**, 3069–3075.
- 12 A. N. Aleshin, J. Y. Lee, S. W. Chu, J. S. Kim and Y. W. Park, *Appl. Phys. Lett.*, 2004, **84**, 5383–5385.
- 13 R. W. I. de Boer, T. M. Klapwijk and A. F. Morpurgo, *Appl. Phys. Lett.*, 2003, **83**, 4345–4347.
- 14 M. Watanabe, Y. J. Chang, S.-W. Liu, T.-H. Chao, K. Goto, Md. M. Islam, C.-H. Yuan, Y.-T. Tao, T. Shinmyozu and T. J. Chow, *Nat. Chem.*, 2012, **4**, 574–578.

- 15 L.-L. Chua, J. Zaumseil, J.-F. Chang, E. C.-W. Ou, P. K.-H. Ho, H. Sirringhaus and R. H. Friend, *Nature*, 2005, **434**, 194–199.
- 16 N.-K. Kim, D. Khim, Y. Xu, S.-H. Lee, M. Kang, J. Kim, A. Facchetti, Y.-Y. Noh and D.-Y. Kim, *ACS Appl. Mater. Interfaces*, 2014, **6**, 9614–9621.
- 17 M. Gsänger, D. Bialas, L. Huang, M. Stolte and F. Würthner, *Adv. Mater.*, 2016, **28**, 3615–3645.
- 18 U. H. F. Bunz and J. Freudenberg, *Acc. Chem. Res.*, 2019, **52**, 1575–1587.
- 19 J.-H. Dou, Y.-Q. Zheng, Z.-F. Yao, Z.-A. Yu, T. Lei, X. Shen, X.-Y. Luo, J. Sun, S.-D. Zhang, Y.-F. Ding, G. Han, Y. Yi, J.-Y. Wang and J. Pei, *J. Am. Chem. Soc.*, 2015, **137**, 15947–15956.
- 20 G. Schweicher, G. Garbay, R. Jouclas, F. Vibert, F. Devaux and Y. H. Geerts, *Adv. Mater.*, 2020, 1905909.
- 21 H. Okamoto, N. Kawasaki, Y. Kaji, Y. Kubozono, A. Fujiwara and M. Yamaji, *J. Am. Chem. Soc.*, 2008, **130**, 10470–10471.
- 22 N. Kawasaki, Y. Kubozono, H. Okamoto, A. Fujiwara and M. Yamaji, *Appl. Phys. Lett.*, 2009, **94**, 043310.
- 23 Y. Kaji, N. Kawasaki, X. Lee, H. Okamoto, Y. Sugawara, S. Oikawa, A. Ito, H. Okazaki, T. Yokoya, A. Fujiwara and Y. Kubozono, *Appl. Phys. Lett.*, 2009, **95**, 183302.
- 24 R. Eguchi, X. He, S. Hamao, H. Goto, H. Okamoto, S. Gohda, K. Sato and Y. Kubozono, *Phys. Chem. Chem. Phys.*, 2013, **15**, 20611–20617.
- 25 Y. Sugawara, Y. Kaji, K. Ogawa, R. Eguchi, S. Oikawa, H. Gohda, A. Fujiwara and Y. Kubozono, *Appl. Phys. Lett.*, 2011, **98**, 013303.

- 26 Y. Sugawara, K. Ogawa, H. Goto, S. Oikawa, K. Akaike, N. Komura, R. Eguchi, Y. Kaji, S. Gohda and Y. Kubozono, *Sensors and Actuators B*, 2012, **171–172**, 544–549.
- 27 Y. Kubozono, X. He, S. Hamao, K. Teranishi, H. Goto, R. Eguchi, T. Kambe, S. Gohda and Y. Nishihara, *Eur. J. Inorg. Chem.*, 2014, 3806–3819.
- 28 H. Okamoto, R. Eguchi, S. Hamao, H. Goto, K. Gotoh, Y. Sakai, M. Izumi, Y. Takaguchi, S. Gohda and Y. Kubozono, *Sci. Rep.*, 2014, **4**, 5330.
- 29 Y. Shimo, T. Mikami, S. Hamao, H. Goto, H. Okamoto, R. Eguchi, S. Gohda, Y. Hayashi and Y. Kubozono, *Sci. Rep.*, 2016, **6**, 21008.
- 30 H. Okamoto, S. Hamao, R. Eguchi, H. Goto, Y. Takabayashi, P. Y-H. Yen, L. U. Liang, C-W. Chou, G. Hoffmann, S. Gohda, H. Sugino, Y-F. Liao, H. Ishii and Y. Kubozono, *Sci. Rep.*, 2019, **9**, 4009.
- 31 A. A. Ruzaiqi, H. Okamoto, Y. Kubozono, U. Zschieschang, H. Klauk, P. Baran and H. Gleskova, *Org. Electron.*, 2019, **73**, 286–291.
- 32 E. Pompei, C. Turchetti, S. Hamao, A. Miura, H. Goto, H. Okamoto, A. Fujiwara, R. Eguchi and Y. Kubozono, *J. Mater. Chem. C*, 2019, **7**, 6022–6033.
- 33 N. Kawai, R. Eguchi, H. Goto, K. Akaike, Y. Kaji, T. Kambe, A. Fujiwara and Y. Kubozono, *J. Phys. Chem. C*, 2012, **116**, 7983–7988.
- 34 X. He, S. Hamao, R. Eguchi, H. Goto, Y. Yoshida, G. Saito and Y. Kubozono, *J. Phys. Chem. C*, 2014, **118**, 5284–5293.
- 35 Y. Shimo, T. Mikami, H. T. Murakami, S. Hamao, H. Goto, H. Okamoto, S. Gohda, K. Sato, A. Cassinese, Y. Hayashi and Y. Kubozono, *J. Mater. Chem. C*, 2015, **3**, 7370–7378.

- 36 H. Inokuchi, G. Saito, P. Wu, K. Seki, T. B. Tang, T. Mori, K. Imaeda, T. Enoki, Y. Higuchi, K. Inaka and N. Yasuoka, *Chem. Lett.*, 1986, **15**, 1263–1266.
- 37 K. Takimiya, I. Osaka, T. Mori and M. Nakano, *Acc. Chem. Res.*, 2014, **47**, 1493–1502.
- 38 H. Ebata, T. Izawa, E. Miyazaki, K. Takimiya, M. Ikeda, H. Kuwabara and T. Yui, *J. Am. Chem. Soc.*, 2007, **129**, 15732–15733.
- 39 Y. Yuan, G. Giri, A. L. Ayzner, A. P. Zoombelt, S. C. B. Mannsfeld, J. Chen, D. Nordlund, M. F. Toney, J. Huang and Z. Bao, *Nat. Commun.*, 2014, **5**, 3005.
- 40 H. Okamoto, S. Hamao, H. Goto, Y. Sakai, M. Izumi, S. Gohda, Y. Kubozono and R. Eguchi, *Sci. Rep.*, 2014, **4**, 5048.
- 41 M. Murai, H. Maekawa, S. Hamao, Y. Kubozono, D. Roy and K. Takai, *Org. Lett.*, 2015, **17**, 708–711.
- 42 A. C. Larson and R. B. Von Dreele, *Los Alamos National Laboratory Report LAUR* **2004**, 86–748.
- 43 N. Kawasaki, W. L. Kalb, T. Mathis, Y. Kaji, R. Mitsuhashi, H. Okamoto, Y. Sugawara, A. Fujiwara, Y. Kubozono, and B. Batlogg, *Appl. Phys. Lett.*, 2008, **93**, 033316.
- 44 F. B. Mallory and C. W. Mallory, *Org. React.*, 1984, **30**, 1–456.
- 45 R. G. Harvey, J. Pataki, C. Cortez, P. D. Raddo and C. X. Yang, *J. Org. Chem.*, 1991, **56**, 1210–1217.
- 46 A. Fürstner and V. Mamane, *J. Org. Chem.*, 2002, **67**, 6264–6267.
- 47 X. He, R. Eguchi, H. Goto, E. Uesugi, S. Hamao, Y. Takabayashi and Y. Kubozono, *Org. Electron.*, 2013, **14**, 1673–1682.

Table 1. Lattice parameters of crystals of [7]phenacene and (C₁₄H₂₉)₂-[7]phenacene

	<i>a</i> [Å]	<i>b</i> [Å]	<i>c</i> [Å]	<i>β</i> [°]
[7]phenacene ^a	8.4381(8)	6.1766(6)	17.829(2)	93.19(1)
(C ₁₄ H ₂₉) ₂ - [7]phenacene	13.1749(4)	5.5116(5)	45.216(3)	95.230(4)

^a Taken from Ref. 47.

Table 2. Lattice parameters (C₁₄H₂₉)₂-[7]phenacene on Au(111) of different structures

	<i>Unit Cell</i> ^a				<i>Relative Orientation</i> ^a			
	<i>a'</i> [Å]	<i>b'</i> [Å]	<i>α'</i> [°]	<i>Area</i> [nm ²]	<i>β'_A</i> [°]	<i>γ'_A</i> [°]	<i>β'_B</i> [°]	<i>γ'_B</i> [°]
Structure 1	35.8	18.9	76	6.6	5	30	-22	-30
Structure 2	39.6	16.5	84	6.5	5	23	-21	-27
Structure 3	37.5	16.7	89	6.2	5	25	-20	-25

^a Parameters of unit cell and relative orientation are shown in Figure 7(a). Subscripts A and B in the parameters for relative orientation refer to the molecules A and B drawn in Figure 7(a). The parameters are obtained from the STM images recorded in different areas (Structure 1, Structure 2 and Structure 3 (not shown in Figure 7(a))).

Table 3. FET parameters of (C₁₄H₂₉)₂-[7]phenacene thin-film FET with SiO₂ gate dielectric, determined from the forward transfer curves

sample	μ (cm ² V ⁻¹ s ⁻¹)	$ V_{th} $ (V)	ON/OFF	S (V decade ⁻¹)	L (μ m)	W (μ m)
#1	1.99	30.2	9.7×10 ⁶	2.1	50	300
#2	2.03 ^a	24.9	1.5×10 ⁶	2.0	100	500
#3	1.51	20.7	8.3×10 ⁵	4.1	150	500
#4	1.65	27.5	2.0×10 ⁷	2.1	250	500
#5	1.84	22.3	9.5×10 ⁶	2.2	285	500
#6	1.21	21.3	8.8×10 ⁶	1.8	350	500
#7	1.36	6.91	1.3×10 ⁴	7.1	600	500
#8	1.49	21.6	1.2×10 ⁷	1.6	450	1000
#9	1.47	19.73	1.0×10 ⁷	2.7	450	1000
average	1.6(3)	22(7)	8(6)×10 ⁶	3(2)		

^a The μ value for device #2 was evaluated to be 1.40 cm² V⁻¹ s⁻¹ from the output curves (see text).

Table 4. FET parameters of [7]phenacene thin-film FET with SiO₂ gate dielectric, determined from the forward transfer curves

sample	μ (cm ² V ⁻¹ s ⁻¹)	$ V_{th} $ (V)	ON/OFF	S (V decade ⁻¹)	L (μ m)	W (μ m)
#1	3.1×10 ⁻¹	39.5	1.3×10 ⁷	3.05	100	800
#2	3.3×10 ⁻¹	59.3	5.7×10 ⁶	2.98	150	800
#3	7.5×10 ⁻¹	41.4	3.7×10 ⁷	2.89	100	500
#4	5.1×10 ⁻¹	48.7	2.6×10 ⁷	3.67	150	500
#5	9.2×10 ⁻¹	66.1	1.9×10 ⁶	3.74	200	500
#6	4.4×10 ⁻¹	50.9	6.2×10 ⁶	3.63	250	500
#7	4.1×10 ⁻¹	55.9	1.4×10 ⁶	2.93	350	500
#8	5.8×10 ⁻¹	39.1	8.8×10 ⁶	3.16	450	500
average	5(2)×10 ⁻¹	50(10)	1(1)×10 ⁷	3.3(4)		

Table 5. FET parameters of (C₁₄H₂₉)₂-[7]phenacene thin-film FET with ZrO₂ gate dielectric, determined from the forward transfer curves

sample	μ (cm ² V ⁻¹ s ⁻¹)	$ V_{th} $ (V)	ON/OFF	S (V decade ⁻¹)	L (μ m)	W (μ m)
#1	7.86×10^{-2}	8.6	7.8×10^5	6.1×10^{-1}	50	300
#2	1.15×10^{-1}	8.3	6.3×10^5	4.5×10^{-1}	100	300
#3	6.07×10^{-2}	2.8	4.3×10^4	6.4×10^{-1}	350	500
#4	7.52×10^{-2}	7.3	1.4×10^5	3.9×10^{-1}	600	500
#5	2.15×10^{-1}	6.4	1.1×10^6	3.8×10^{-1}	450	1000
#6	1.06×10^{-1}	6.7	5.7×10^5	6.8×10^{-1}	450	1000
#7	1.53×10^{-1}	5.5	9.1×10^5	1.03	450	1000
average	$1.1(5) \times 10^{-1}$	7(2)	$6(4) \times 10^5$	$6(2) \times 10^{-1}$		

Table 6. FET parameters of (C₁₄H₂₉)₂-[7]phenacene thin-film FET with EDL capacitor, determined from the forward and reverse transfer curves

sample		μ (cm ² V ⁻¹ s ⁻¹) ^a	$ V_{th} $ (V)	ON/OFF	S (V decade ⁻¹)	L (μ m)	W (μ m)
#1	F	8.26×10^{-1}	2.00	1.3×10^3	2.78×10^{-1}	150	567
	R	3.51×10^{-1}	1.66	2.8×10^2	5.99×10^{-1}		
#2	F	7.97×10^{-1}	2.27	9.9×10^3	2.21×10^{-1}	150	387
	R	1.98×10^{-1}	1.75	2.8×10^2	1.71×10^{-1}		
#3	F	1.25	2.40	2.2×10^2	2.99×10^{-1}	150	525
	R	3.21×10^{-1}	1.93	1.9×10^2	8.76×10^{-2}		
#4	F	1.02	2.17	1.1×10^4	2.73×10^{-1}	100	600
	R	2.85×10^{-1}	1.80	2.7×10^2	1.62×10^{-1}		
#5	F	1.00	2.46	8.0×10^3	1.13×10^{-1}	100	319
	R	2.34×10^{-1}	2.02	3.3×10^2	1.34×10^{-1}		
#6	F	8.22×10^{-1}	2.34	2.4×10^3	8.98×10^{-2}	100	263
	R	2.24×10^{-1}	1.99	5.4×10^2	5.67×10^{-1}		
average	F	1.0(2)	2.3(2)	$6(5) \times 10^3$	$2.1(9) \times 10^{-1}$		
	R	$2.7(6) \times 10^{-1}$	1.9(1)	$3(1) \times 10^2$	$3(2) \times 10^{-1}$		
average		$6(4) \times 10^{-1}$	2.1(3)	$3(4) \times 10^3$	$3(1) \times 10^{-1}$		

^a F and R refer to the FET parameters evaluated from the forward and reverse transfer curves.

Figure captions

Scheme 1 Synthetic route to $(C_{14}H_{29})_2$ -[7]phenacene.

Fig. 1 Molecular structures of alkyl-substituted phenacenes.

Fig. 2 Device structures of $(C_{14}H_{29})_2$ -[7]phenacene thin-film FETs with (a) a solid gate dielectric and (b) an EDL capacitor using ionic liquid, bmim[PF₆].

Fig. 3 ¹H NMR spectra (600 MHz, CDCl₂CDCl₂) of $(C_{14}H_{29})_2$ -[7]phenacene (lower, 80°C) and [7]phenacene (upper, 75°C).

Fig. 4 Absorption and fluorescence spectra of $(C_{14}H_{29})_2$ -[7]phenacene (yellow line) and [7]phenacene (blue line) in CHCl₃ at room temperature (r.t.).

Fig. 5 XRD pattern of (a) polycrystalline $(C_{14}H_{29})_2$ -[7]phenacene sample and (b) thin film of $(C_{14}H_{29})_2$ -[7]phenacene formed on an SiO₂/Si substrate. In (a), experimental XRD pattern (black cross) of polycrystalline $(C_{14}H_{29})_2$ -[7]phenacene, together with the pattern (red solid line) calculated by LeBail fitting. The red ticks refer to positions of $(C_{14}H_{29})_2$ -[7]phenacene. The blue solid line corresponds to the difference between the experimental XRD pattern and the calculated one. Inset of (b): expanded XRD pattern for 002 and 003 reflections. (c) Orientation of the long axis of the $(C_{14}H_{29})_2$ -[7]phenacene molecule with respect to c^* axis (normal to ab plane) in the thin film formed on an SiO₂/Si substrate.

Fig. 6 (a) UV-vis and (b) PYS spectra of thin films of $(C_{14}H_{29})_2$ -[7]phenacene. The thin films were formed on quartz glass and Au/SiO₂/Si substrate. (c) Schematic representation of energy levels of $(C_{14}H_{29})_2$ -picene, $(C_{14}H_{29})_2$ -[6]phenacene, $(C_{14}H_{29})_2$ -[7]phenacene and [7]phenacene.

Fig. 7 (a) STM image and (b) STS of $(C_{14}H_{29})_2$ -[7]phenacene monolayer formed on an Au substrate. In (a), the STM image was recorded at a sample bias voltage (V_s) of -50 mV. The observed area refers to ‘Structure 1’. The symbols (a' , b' , α' , β' , γ' , δ' and ε') shown in (a) correspond to the parameters of the unit cell and its relative orientation listed in Table 2. Two types of molecules located at (0,0) and (1/2,1/2) are named ‘Molecule A’ and ‘Molecule B’, respectively. It should be noted that the definition of unit cell parameters (a' , b' and α') employed in the STM image is different from that determined from XRD. In set (a), the STM image was recorded at V_s of -2.5 V. The observed area refers to ‘Structure 2’. In (b), the red and blue curves refer to the dI/dV – voltage (V_s) plots measured on alkyl-chains and π -framework (benzene core) of $(C_{14}H_{29})_2$ -[7]phenacene. (c) XRD pattern of $(C_{14}H_{29})_2$ -[7]phenacene thin film formed on an Au substrate. Inset of (c): expanded XRD pattern for 002, 003 and 004 reflections.

Fig. 8 (a) Transfer and (b) output curves of a $(C_{14}H_{29})_2$ -[7]phenacene thin-film FET with an SiO₂ gate dielectric. This FET refers to device #2 in Table 3; $L = 100$ μm and $W = 500$ μm . (c) Transfer and (d) output curves of a [7]phenacene thin-film FET with an SiO₂ gate dielectric. This FET refers to device #5 in Table 4; $L = 200$ μm and $W = 500$ μm .

Fig. 9 (a) Transfer and (b) output curves of $(C_{14}H_{29})_2$ -[7]phenacene thin-film FET with a ZrO_2 gate dielectric. This FET refers to device #5 in Table 5; $L = 450 \mu\text{m}$ and $W = 1000 \mu\text{m}$.

Fig. 10 (a) Transfer and (b) output curves of a $(C_{14}H_{29})_2$ -[7]phenacene thin-film EDL FET. This FET refers to device #3 in Table 6; $L = 150 \mu\text{m}$ and $W = 525 \mu\text{m}$.

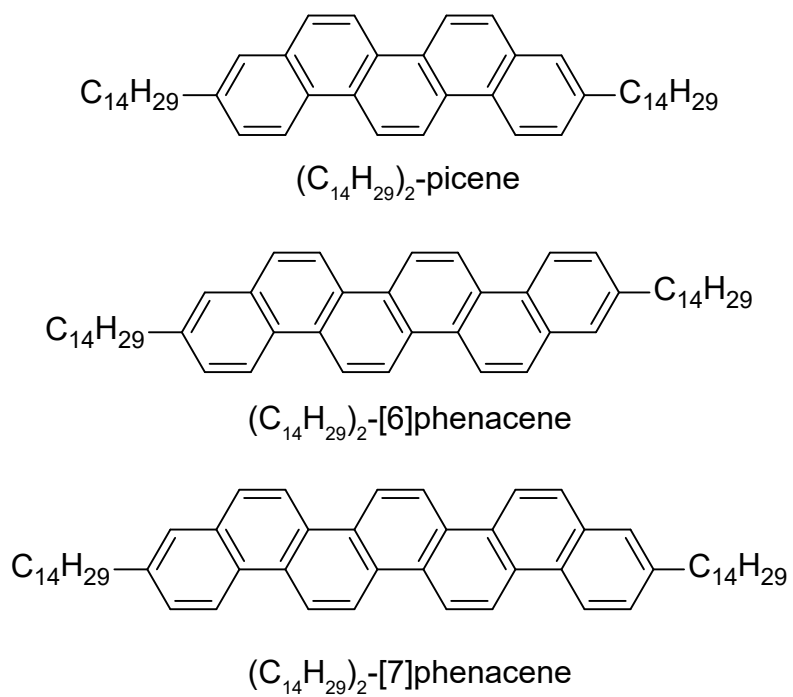


Fig. 1 Okamoto *et al.*

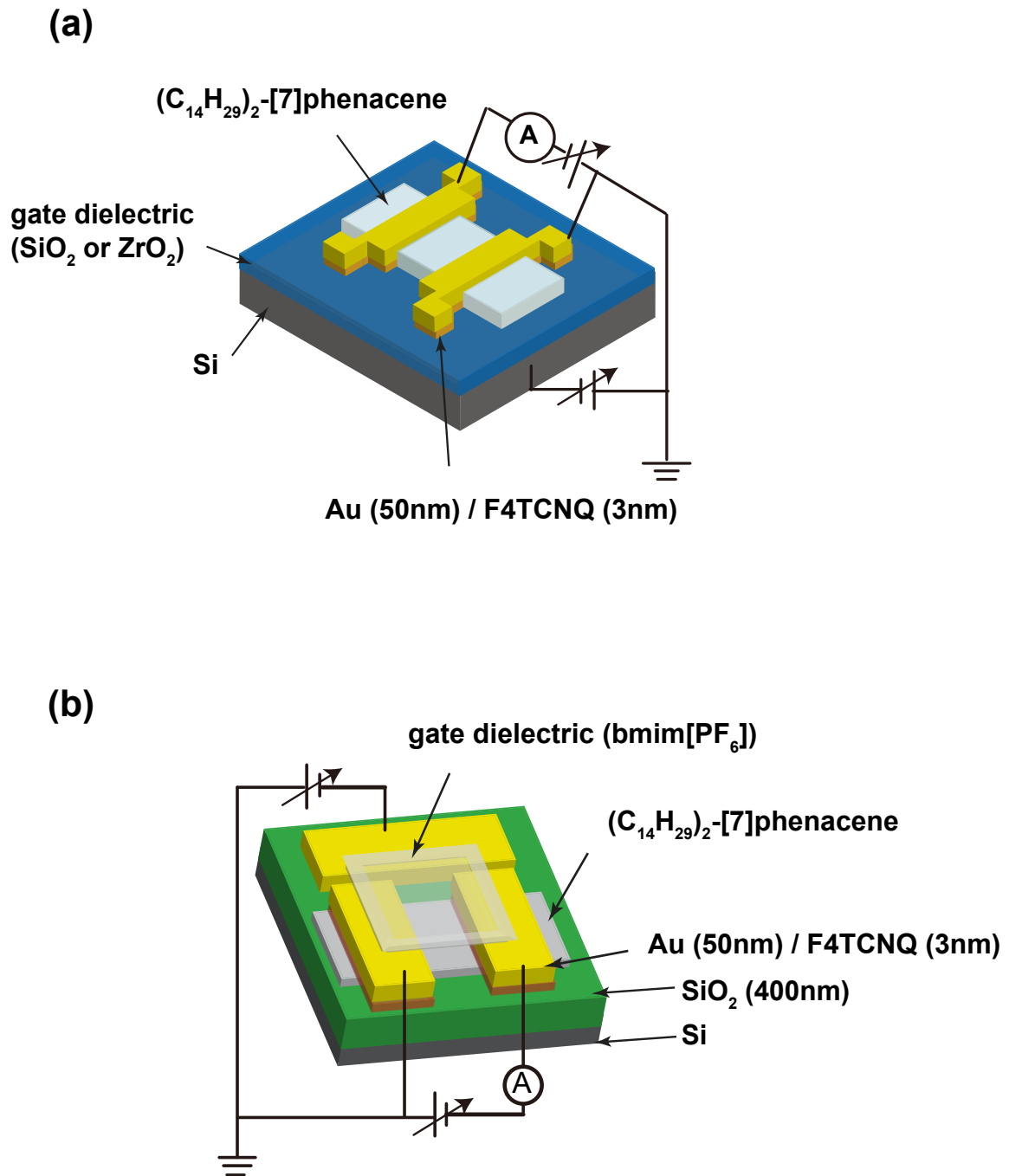
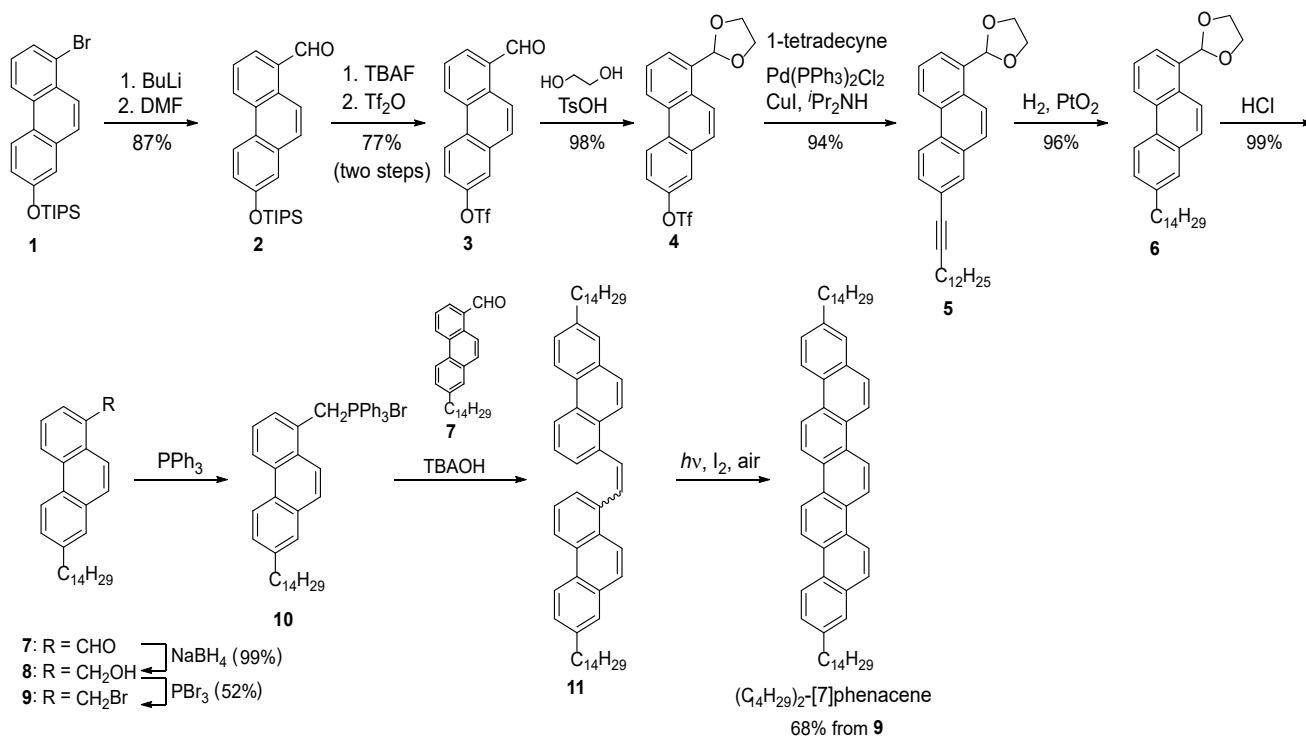


Fig. 2 Okamoto *et al.*

Scheme 1. Okamoto *et al.*

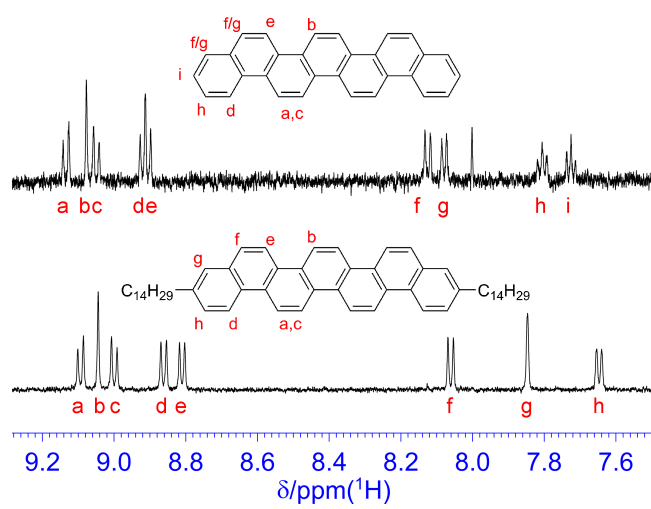


Fig. 3 Okamoto *et al.*

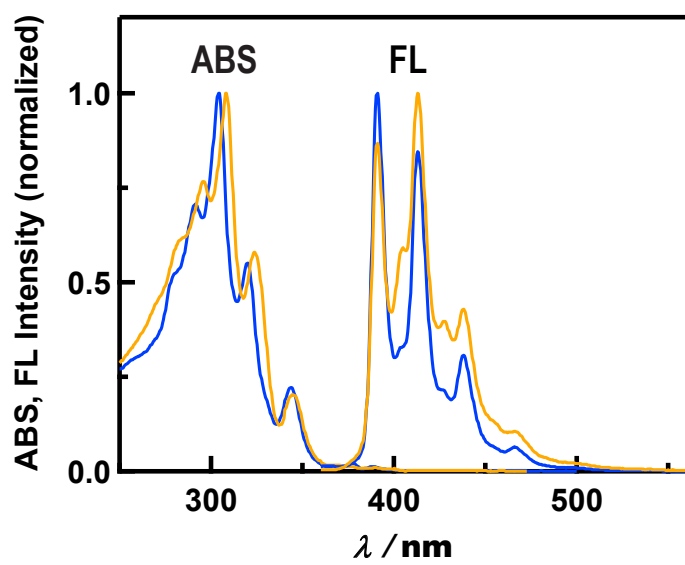


Fig. 4 Okamoto *et al.*

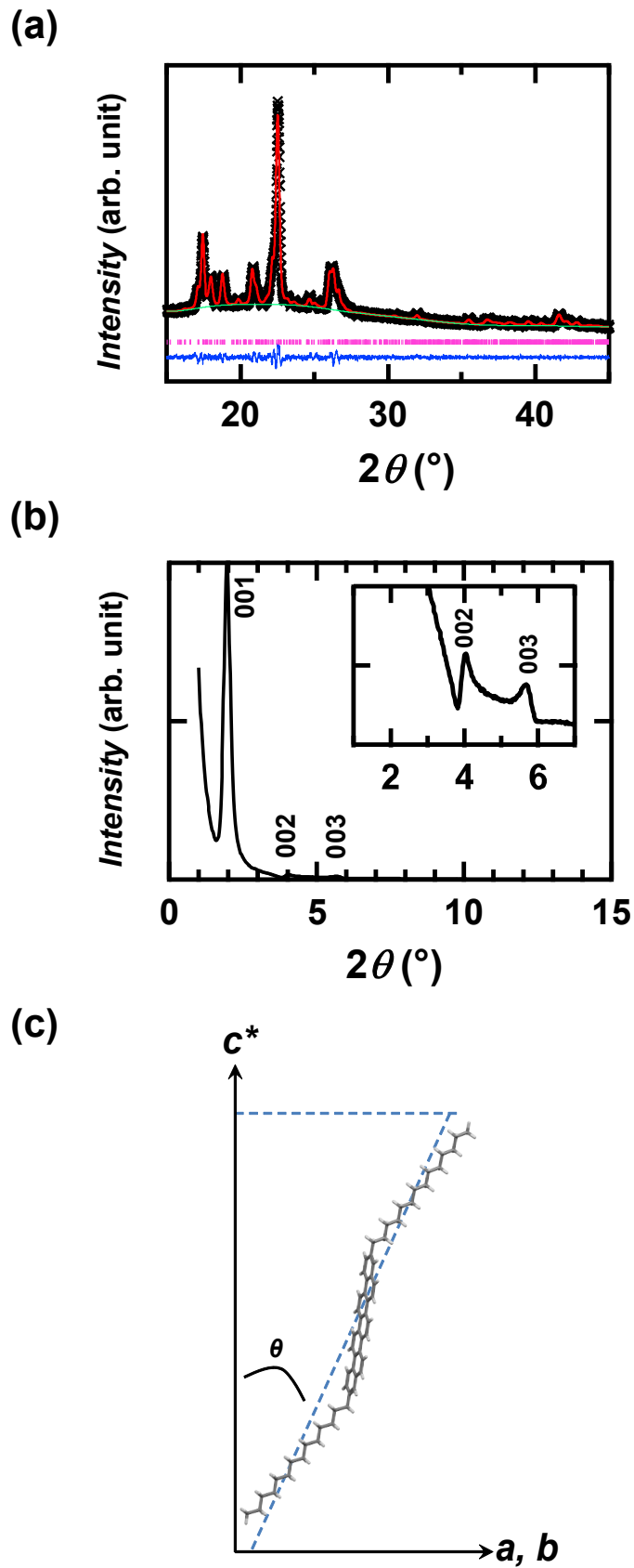
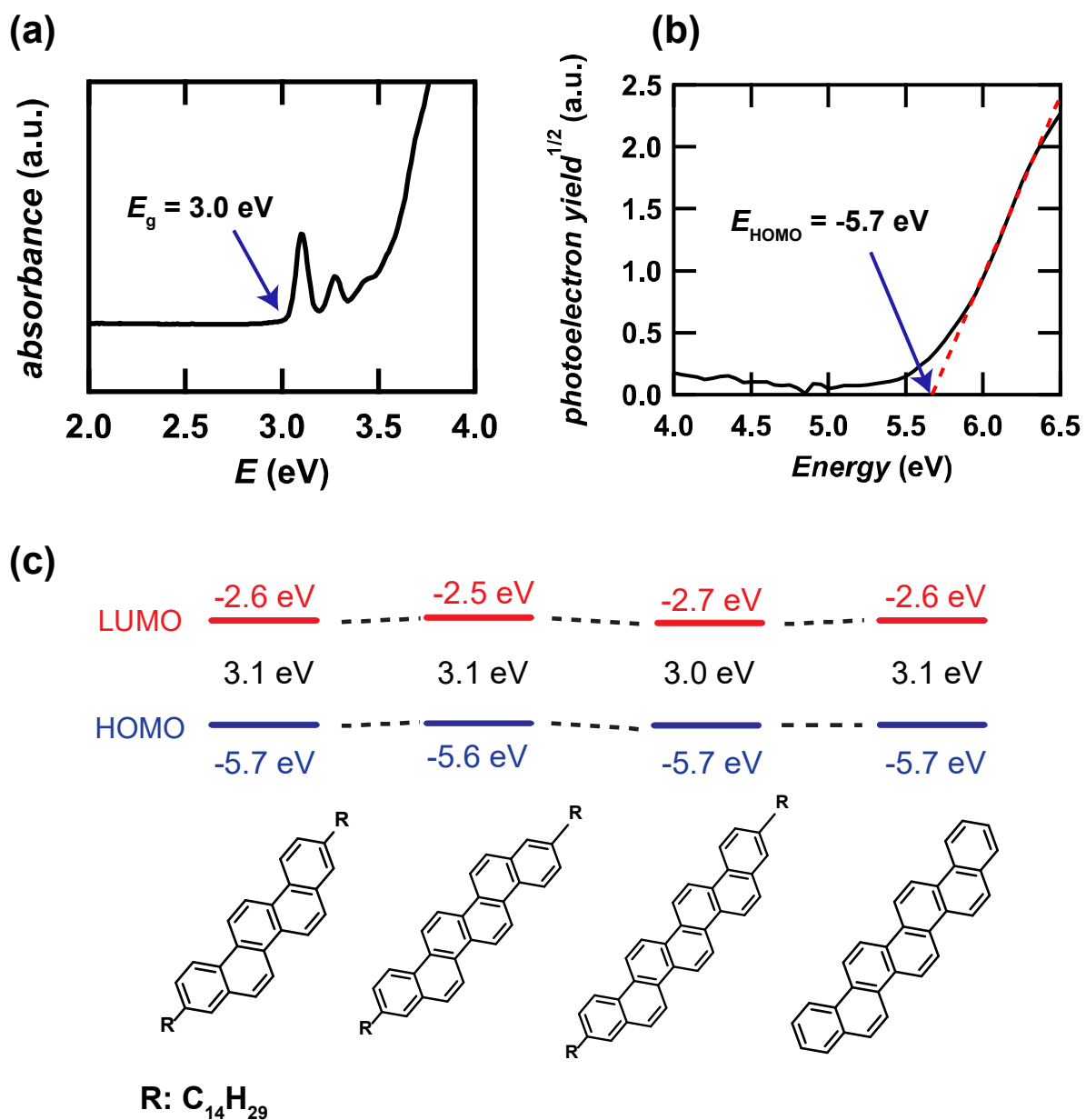
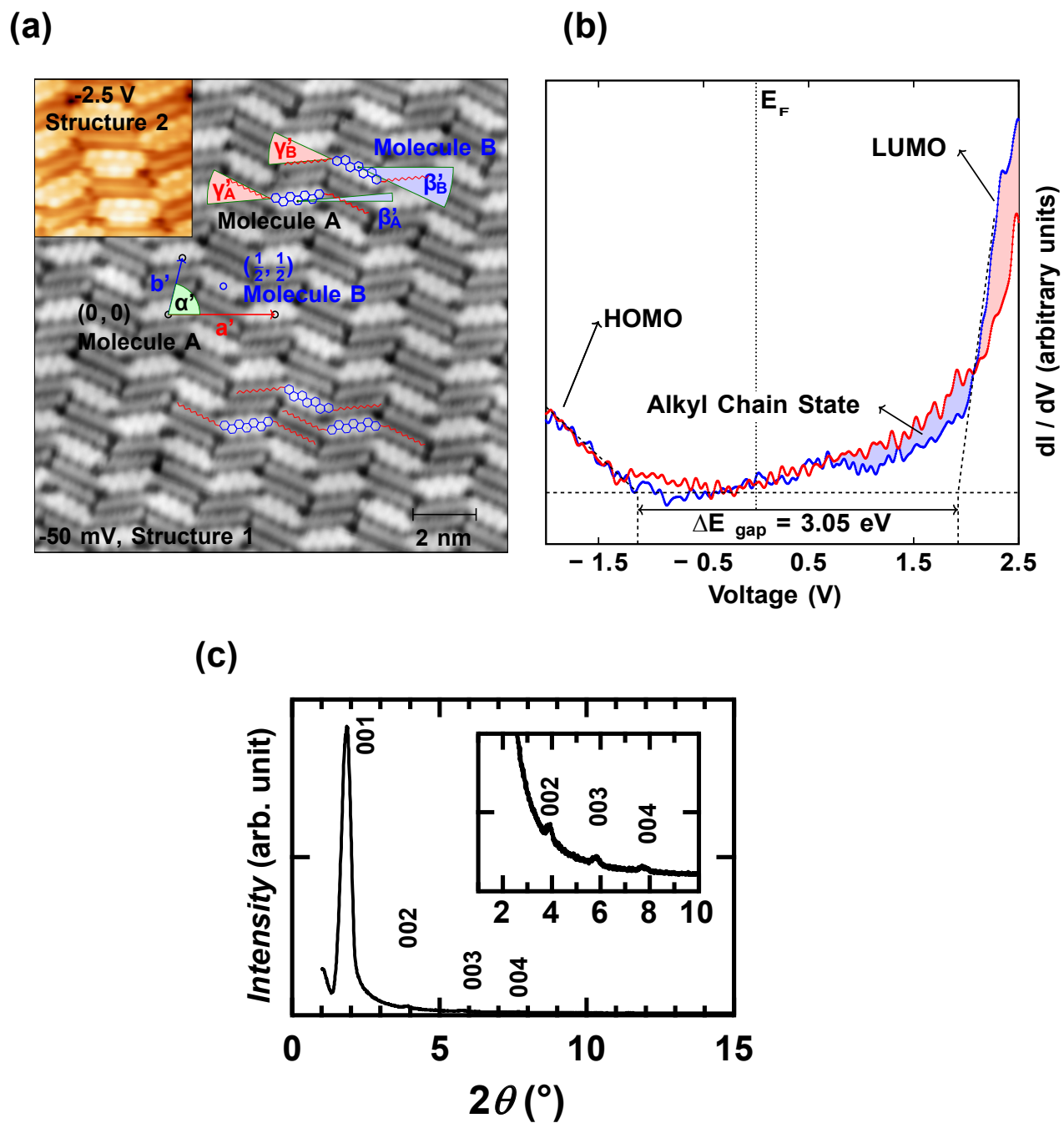


Fig. 5 Okamoto *et al.*

Fig. 6 Okamoto *et al.*

Fig. 7 Okamoto *et al.*

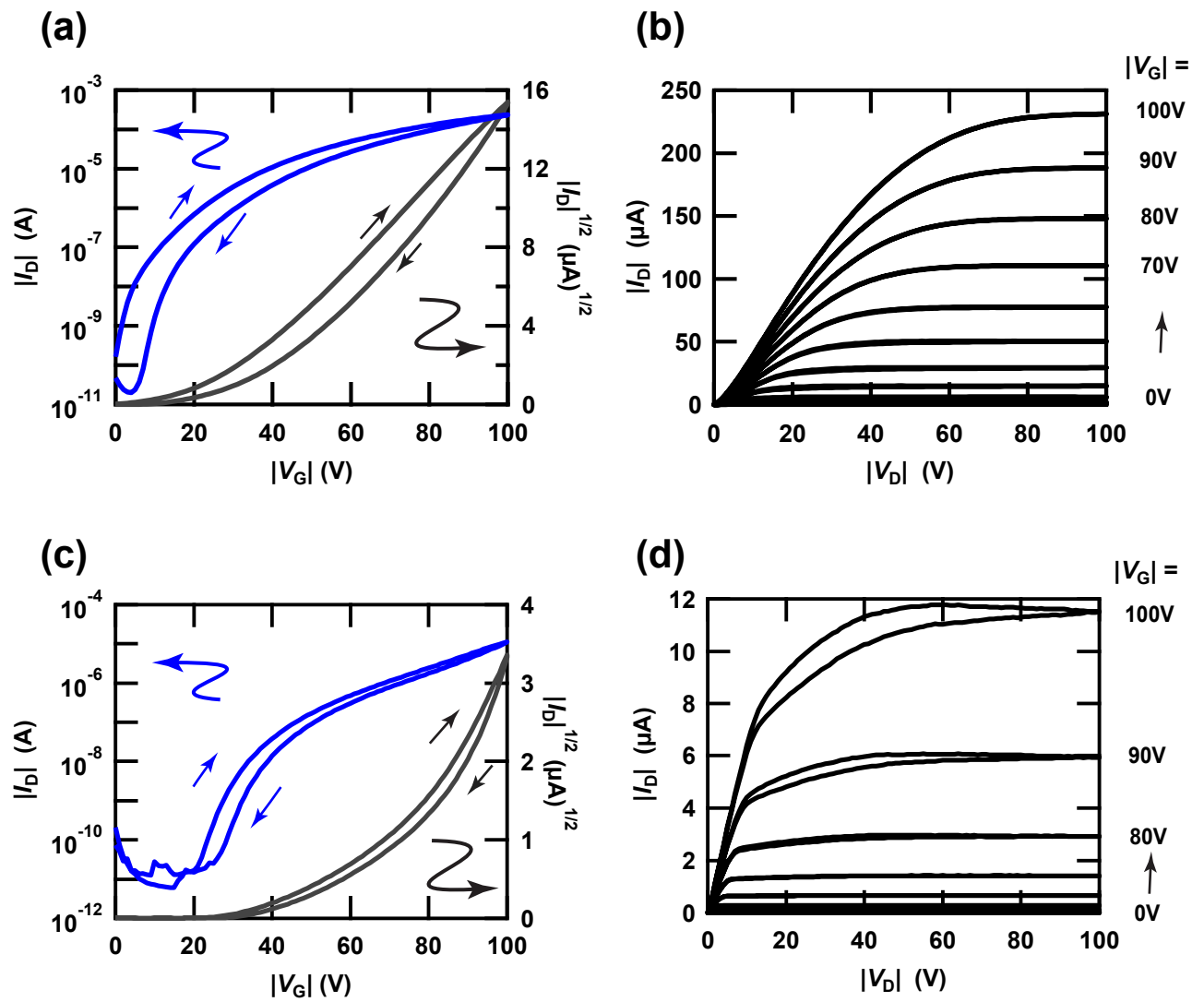


Figure 8. Okamoto *et al.*

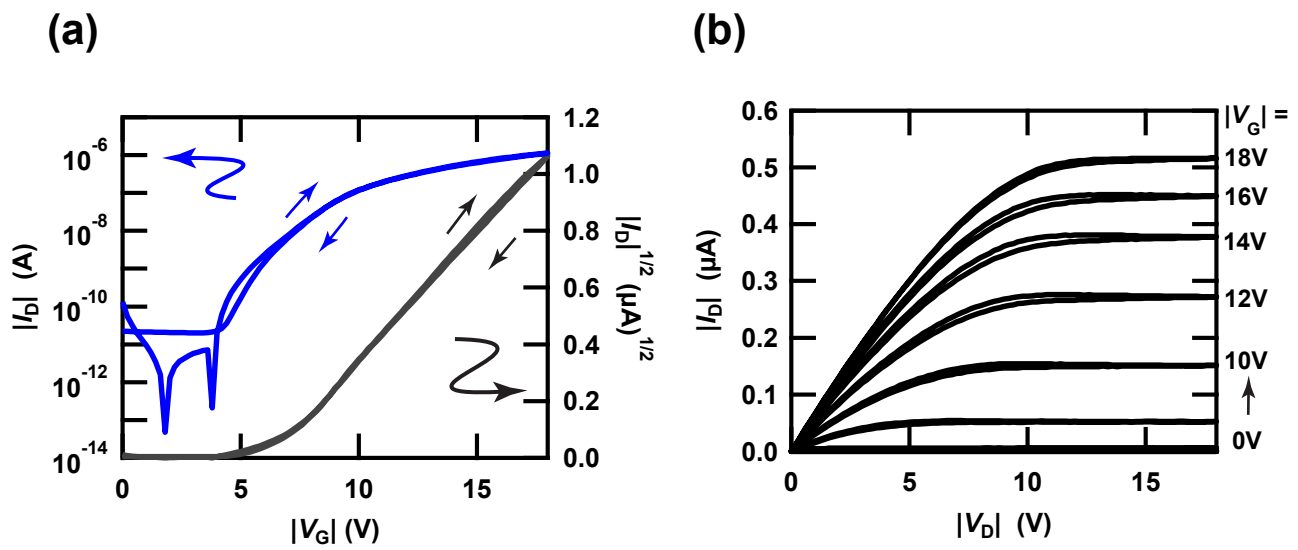


Fig. 9 Okamoto *et al.*

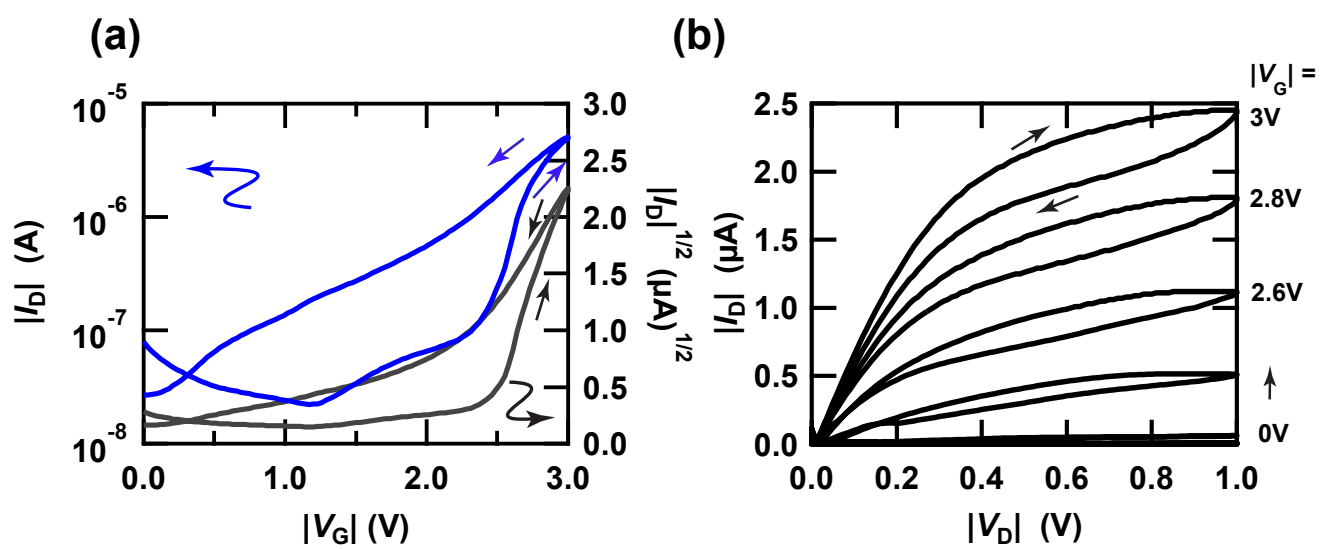


Fig. 10 Okamoto *et al.*

Table of Contents Entry

Ditetradecyl-substituted [7]phenacene was prepared and applied to thin-film FET devices displaying higher mobility compared to parent [7]phenacene.

